

Antispiral Waves in Reaction-Diffusion Systems

Yunfan Gong¹ and David J. Christini^{1,2,*}

¹*Division of Cardiology, Department of Medicine, Weill Medical College of Cornell University, New York, New York 10021*

²*Department of Physiology and Biophysics, Weill Graduate School of Medical Sciences of Cornell University, New York, New York 10021*

(Received 25 March 2002; revised manuscript received 5 July 2002; published 26 February 2003)

We report spontaneous antispiral wave formation in typical reaction-diffusion systems. Our findings qualitatively reproduce a series of phenomena recently observed in a Belousov-Zhabotinsky-type chemical reaction. We found that antispiral waves can occur only near the Hopf bifurcation, when the system is characterized by small amplitude oscillatory (as opposed to excitable) dynamics. For reaction-diffusion systems in the vicinity of the Hopf bifurcation, the specific conditions required for antispiral formation are established here through theoretical analyses and numerical simulations. Thus, this work provides a comprehensive description of the mechanisms underlying antispiral waves in reaction-diffusion systems.

DOI: 10.1103/PhysRevLett.90.088302

PACS numbers: 82.40.Ck, 05.45.-a, 47.54.+r, 89.75.Kd

In recent years, spatiotemporal pattern formation in systems driven away from equilibrium has been extensively investigated theoretically and experimentally [1]. Among a wide variety of patterns studied, spiral waves, which occur in biological systems and inorganic processes, seem to be of particular importance and interest [2]. The propagation direction of spiral waves did not receive much attention until a recent observation of inwardly rotating spirals, termed *antispirals*, in the Belousov-Zhabotinsky (BZ) reaction dispersed in water droplets of a water-in-oil aerosol OT (AOT) microemulsion (BZ-AOT system) [3]. In the BZ-AOT system, Vanag and Epstein found that new waves with high speed first emerge at the boundary between the basins of adjacent antispirals, then split and move slowly toward their centers, where they annihilate [3].

In a series of recent studies, Vanag and Epstein explored the origin of antispirals. First, they produced antispirals using a ring-shaped apparatus with different diffusion coefficients for the activator variable on the inner circle and the outer annulus [3]. In a succeeding paper on pattern formation in the BZ-AOT system [4], they developed a four-variable model to explain *accelerating waves*—waves that rush to fill the vacancy left by receding waves of neighboring antispirals. More recently, using perturbation techniques they generated inwardly propagating concentric waves or antipacemakers [5] that were similar to those found by Zhang *et al.* [6]. While these studies illuminated some aspects of antispiral waves, the fact that three completely different models were used to explain the dynamics [3–5] indicates that the mechanism of spontaneous antispiral formation is still unclear.

It is well known that the geometrical shape of a wave front is among many factors that determine its conduction velocity C . In an excitable medium, this relationship for wave fronts at small curvatures ($1/r$) is specified by the classic eikonal equation,

$$C(r) = c - \frac{D}{r}, \quad (1)$$

where c is the constant conduction velocity of a plane wave, and D is the diffusion coefficient of the fast-changing activator variable of the medium. In deriving the above formula [7,8], one of the key assumptions for the typical excitable medium, as exemplified by the FitzHugh-Nagumo (FHN) model [9],

$$\begin{aligned} \partial u / \partial t &= (u - u^3/3 - v)/\epsilon + D_u \nabla^2 u, \\ \partial v / \partial t &= u - \gamma v + \delta + D_v \nabla^2 v, \end{aligned} \quad (2)$$

is a very small ratio ϵ ($0 < \epsilon \ll 1$) between the fast excitation rate and the slow recovery rate. As a consequence of this assumption, the dynamics are excitable and the system behaves like a relaxation oscillator; that is, the motion is highly inharmonic with asymmetric alternating fast and slow variations [Fig. 1(a)]. Furthermore, under this assumption, spiral waves are characterized by wide activation pulses with sharply rising fronts in space, as shown in Fig. 1(b). However, if the assumption is not true, as in the following cases in which the systems approach the Hopf bifurcation and the dynamics are harmonically oscillatory rather than excitable, then Eq. (1) will no longer hold [12,13], and in real systems, new patterns may emerge [3].

The prototype of an oscillatory medium close to the Hopf bifurcation point is the complex Ginzburg-Landau (CGL) equation [14],

$$\frac{\partial W}{\partial t} = W - (1 + i\alpha)W|W|^2 + (1 + i\beta)\nabla^2 W, \quad (3)$$

where i is the imaginary unit and $\nabla^2 = (\partial^2/\partial x^2) + (\partial^2/\partial y^2)$ denotes the two-dimensional Laplacian operator. Because the CGL system is near the Hopf bifurcation, the motion is sinusoidal, which is in sharp contrast to the

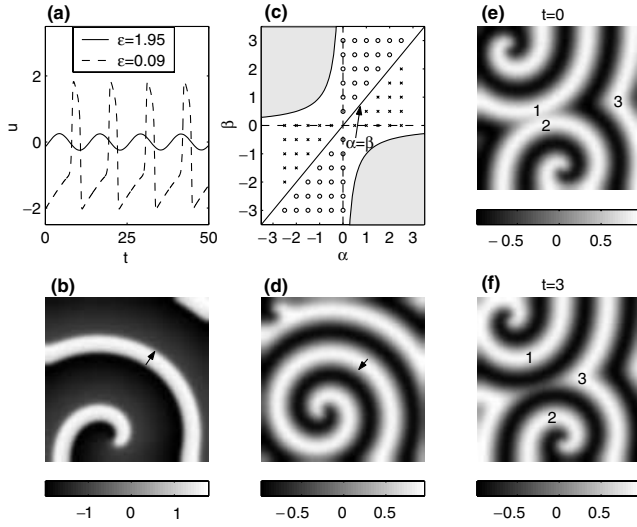


FIG. 1. Spiral and antispiral waves in typical excitable (FHN) and oscillatory (CGL) media. (a) Time history (arbitrary units) of the fast activator variable u of the FHN model. The solid line and the dashed line correspond to the small amplitude, sinusoidal oscillation ($\epsilon = 1.95$) and the large amplitude relaxation oscillation ($\epsilon = 0.09$), respectively. (b) Snapshot of spirals in the FHN model ($\epsilon = 0.09$, $\gamma = 0.5$, $\delta = 0.7$, $D_u = 1.0$, $D_v = 0.0$), where the arrow indicates outward propagation of waves. The spirals were initiated on a 100×100 grid by the cross-field protocol [10]. (c) The parameter plane (α , β) shows where spirals (\circ) and antispirals (\times) exist in the CGL system. The shaded areas indicate where no plane wave can remain stable according to the Benjamin-Feir instability criterion: $1 + \alpha\beta < 0$. Spirals occur when $\beta > \alpha \geq 0$ or $0 \geq \alpha > \beta$; while antispirals occur when $\alpha > \beta \geq 0$ or $0 \geq \beta > \alpha$. On the borderline $\alpha = \beta$, the medium may either support phase waves or remain static, depending on the parameter choice. Points are evenly distributed in the parameter regions $\alpha\beta \geq 0$ with $\alpha \in [-2.5, 2.5]$, $\beta \in [-3, 3]$ and a step size of 0.5. For each point, the CGL system was integrated a total of 4×10^5 steps using the explicit Euler method with time step $\Delta t = 0.005$, and the standard five-point approximation for the Laplacian operator [11] with space step $\Delta x = \Delta y = 0.5$. Spirals or antispirals were spontaneously formed on a 200×200 grid with no-flux boundaries from random initial conditions. The results remain the same when checked with the fourth order Runge-Kutta integrating method. (d) Snapshot of a well-developed single antispiral in the CGL system ($\alpha = -1.5$, $\beta = 0.0$). The arrow indicates inward propagation of waves, which move toward the center. The system was integrated using the same methods as in (c) with time step $\Delta t = 0.01$, space step $\Delta x = \Delta y = 0.5$, and a total of 4×10^5 integration steps. The antispirals were spontaneously formed on a 100×100 grid with no-flux boundaries from random initial conditions. (e)–(f) Snapshots of antispirals in the CGL system ($\alpha = 1.5$, $\beta = 0.0$), where the waves annotated 1, 2, and 3 in (e) propagate to their corresponding positions in (f), demonstrate inwardly propagating antispiral motions.

highly inharmonic motion of the excitable FHN model. When two real parameters α and β vary, the complex field W , which describes the amplitude and phase of pattern modulations, will exhibit rich dynamical behav-

iors including both spirals and antispirals [see Fig. 1(c)]. We note that previous studies of the CGL equation [15–17] did not report antispiral behavior [18].

The specific type of antispiral patterns in the CGL system was dependent on the parameter choice. Figure 1(d) shows a well-developed single antispiral spontaneously formed when $\alpha = -1.5$, $\beta = 0.0$ [19]. Furthermore, accelerating waves were observed along with antispirals in our simulations. On the right side of Fig. 1(e), a new wave (annotated 3) first emerges at the boundary between the basins of two adjacent antispirals, then accelerates [Fig. 1(f)] into the vacant area left by two receding waves (annotated 1 and 2) which move apart and slowly towards the centers of their respective antispirals [similarly, see Fig. 1(b) in [3] and Figs. 3(a)–3(e) in [4]]. These wave behaviors were also observed for antispirals in other reaction-diffusion systems to be discussed below.

It has been shown that wave-propagation direction (outward or inward) is governed by the result of the competition between (spiral or antispiral) waves and their surrounding bulk oscillations [3]. Moreover, spiral or antispiral waves in general behave asymptotically as plane waves far from their cores. Therefore, we hypothesize that the condition for the occurrence of antispirals is that the frequency of the bulk oscillation (Ω_0) is larger than the asymptotic frequency of the (antispiral) wave (Ω_k), i.e., $|\Omega_0| > |\Omega_k|$ [20]. For the CGL system, it is known [1,14,16,21] that $\Omega_0 = \alpha$ and $\Omega_k = \alpha + (\beta - \alpha)k^2$, where k is the wave number. Here, for simplicity, we consider only the case when two real parameters α and β are of the same sign, i.e., $\alpha\beta \geq 0$ [22]. Note $0 \leq k < 1$ [21]; thus from the condition $|\Omega_0| > |\Omega_k|$ the parameter regime where antispirals occur is $\alpha > \beta \geq 0$ or $0 \geq \beta > \alpha$. Similarly, the parameter regime where spirals occur ($|\Omega_0| < |\Omega_k|$) is $\beta > \alpha \geq 0$ or $0 \geq \alpha > \beta$. These theoretical results agree with those from numerical simulations [see Fig. 1(c)].

To further examine these results in other reaction-diffusion systems and to compare with experimental observations in the BZ-AOT system, we consider the aforementioned FHN model of Eq. (2). This system has been widely used to explore spiral-wave behavior in excitable BZ chemical reactions [2]. If, however, the FHN model is in the vicinity of the Hopf bifurcation point, the motion will be sinusoidal with relatively small amplitude oscillations that can form antispirals spontaneously [see Fig. 1(a)]. Because the system undergoes a supercritical ($g' > 0$) Hopf bifurcation, the CGL approximation is valid [14,23]. Following the classic reductive perturbation method [14,23], a unique CGL equation with parameters

$$\begin{aligned} \alpha &= g''/g' = -\frac{\sqrt{\gamma}}{\sqrt{1-\gamma}}, \\ \beta &= d''/d' = \frac{\sqrt{\gamma} D_v - D_u}{\sqrt{1-\gamma} D_v + D_u} \end{aligned} \quad (4)$$

can be defined from the original FHN model by setting $\delta = 0.0$. We observed both spirals and antispirals depending on the parameter values. Of particular interest here is the simplest case when $D_u = D_v$, because according to Eq. (4) the parameter $\beta = 0.0$. When varying the parameter γ of the FHN model in the range $0.2 \leq \gamma \leq 0.8$, from Eq. (4) the corresponding parameter α of the CGL equation changes within the range $-0.5 \leq \alpha \leq -2$. As predicted from the CGL equation [see Fig. 1(c)], in the above parameter region of the FHN model we observed only antispirals. For example, when $\gamma = 0.5$, $D_u = D_v = 0.005$, Eq. (4) gives $\alpha = -1.0$, $\beta = 0.0$. Clearly, these two parameters are within the antispiral regime of the CGL equation given in Fig. 1(c). Consistent with this prediction, a direct numerical simulation of the FHN model ($\epsilon = 1.95$) in the vicinity of the Hopf bifurcation ($\epsilon_c = 2.0$) shows antispirals in Figs. 2(a) and 2(b) [19]. Figures 2(c) and 2(d) exhibit antispiral waves for another case of the FHN model ($\epsilon = 1.30$, $\gamma = 0.75$, and $D_u = D_v = 0.005$) near the Hopf bifurcation ($\epsilon_c = 1.333$), which are also consistent with the CGL prediction with $\alpha = -1.73$, $\beta = 0.0$ from Eq. (4). Furthermore, these antispirals resemble experimental observations in the BZ-AOT system [see Figs. 1(a) and 1(b) in [3]]. Because the system is very close to the Hopf bifurcation, the waves have relatively small amplitude, as observed for small amplitude oscillating *packet waves* in the BZ-AOT system [5]. Note that to generate antispirals spontaneously, the diffusion coefficients in the FHN model (or the Oregonator model below) must be extremely small (~ 0.005) compared with those (~ 1.0) in the excitable case when $0 < \epsilon \ll 1$; otherwise, fast propagating phase waves will dominate the entire medium. Consistent with these model predictions, the diffusion coefficients in the BZ-AOT system were also small (roughly 2 or 3 orders of magnitude smaller than normal, due to the percolation effect) [3,4] when antispirals occurred.

References [3–5] did not specify the type of Hopf bifurcation (subcritical or supercritical) for the BZ-AOT system. For this reason, in addition to the supercritical case described above (CGL equation and the FHN model where the CGL approach is applicable), we investigated the subcritical case using the Oregonator model of the BZ chemical reaction. In dimensionless form, the two-variable version of the Oregonator model is [24,25]

$$\begin{aligned} \frac{\partial u}{\partial t} &= \frac{1}{\epsilon} \left(u - u^2 - f v \frac{u - q}{u + q} \right) + D_u \nabla^2 u, \\ \frac{\partial v}{\partial t} &= u - v + D_v \nabla^2 v, \end{aligned} \quad (5)$$

where the activator variable u and the inhibitor variable v represent the concentrations of the autocatalytic species HBrO_2 and the transition ion catalyst in the oxidized state Ce^{3+} or Fe^{3+} , respectively. The parameter ϵ , which describes different reaction rates for the two variables u and v (and plays a similar role as described earlier for the FHN model), is used as the control parameter. With

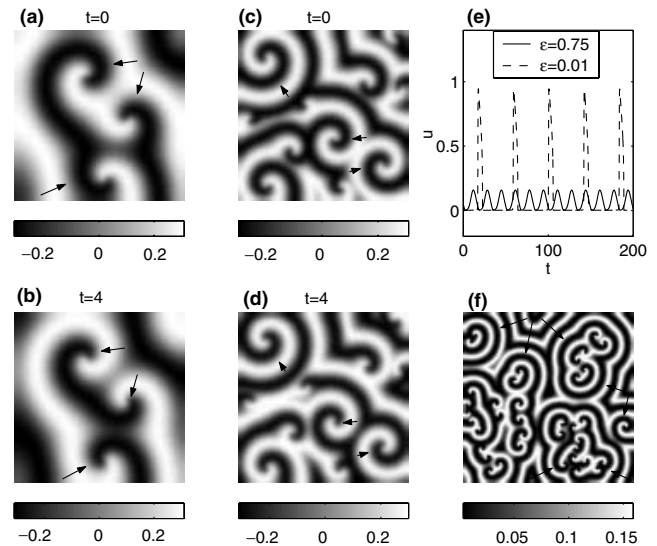


FIG. 2. Antispiral waves in the FHN and the Oregonator models, where the arrows indicate inward propagation of waves. Both models were integrated using the same methods as in Fig. 1(c) with time step $\Delta t = 0.01$, space step $\Delta x = \Delta y = 0.5$, and a total of 5×10^6 integration steps. The antispirals were spontaneously formed on a 100×100 grid with no-flux boundaries from random initial conditions. The results remain qualitatively unchanged when decreasing the time step Δt or increasing the total integration steps. (a),(b) Snapshots of antispirals in the FHN system ($\epsilon = 1.95$, $\gamma = 0.5$, $\delta = 0.0$, $D_u = D_v = 0.005$). (c),(d) Snapshots of antispirals in the FHN system ($\epsilon = 1.3$, $\gamma = 0.75$, $\delta = 0.0$, $D_u = D_v = 0.005$). (e) Time history (arbitrary units) of the activator variable u of the Oregonator model. The solid line and the dashed line correspond to the small amplitude, nearly sinusoidal oscillation ($\epsilon = 0.75$) and the large amplitude relaxation oscillation ($\epsilon = 0.01$), respectively. (f) Snapshot of antispirals in the Oregonator model ($\epsilon = 0.75$, $q = 0.002$, $f = 0.95$, $D_u = D_v = 0.001$).

variation of the parameter ϵ , the system undergoes a subcritical ($g' < 0$) Hopf bifurcation in the oscillatory parameter regime $0.5 < f < 1 - q$ [1]. In this case, the CGL approximation cannot be applied [14,23]—numerical simulation must be used. We set $q = 0.002$, $f = 0.95$. When ϵ is very small, for example, $\epsilon = 0.01$ (which was widely used in previous theoretical studies of the excitable BZ reaction [26]), the system becomes a typical relaxation oscillator with large amplitude, highly inharmonic oscillations [Fig. 2(e)]. The relaxation oscillation closely resembles the large excursion motion of the excitable case [1], in which spiral waves have been extensively investigated previously [27]. If, however, the system is in the vicinity of the Hopf bifurcation point ($\epsilon_c = 0.7782$), the motion will be sinusoidal with relatively small amplitude oscillations that can form antispirals spontaneously [see Fig. 2(e)]. Figure 2(f) exhibits antispiral waves for such a case when $\epsilon = 0.75$, $D_u = D_v = 0.001$ [19]. To spontaneously form antispirals, the diffusion coefficients in the Oregonator model must be extremely small (~ 0.001) compared with those (~ 0.01)

in the excitable case when $\epsilon = 0.01$ [26]. Finally, a direct estimation from numerical simulations of the Oregonator model gives $\omega_0 = 0.3806$, $\omega_k = 0.3770$. The inequality $|\omega_0| > |\omega_k|$, which is established for the occurrence of antispirals in the CGL equation, remains true even when the CGL approximation fails.

Here we have shown antispiral waves spontaneously formed in typical reaction-diffusion systems: the CGL equation, the FHN model, and the Oregonator model of the BZ reaction. Notably, our numerical results are in agreement with a series of observations in recent experiments on the BZ-AOT system [3–5], suggesting a similar mechanism underlying the antispiral phenomenon. Through our theoretical analyses and numerical simulations, the condition required for reaction-diffusion systems close to the Hopf bifurcation (whether supercritical as in the FHN model or subcritical as in the Oregonator model) to form antispirals is now determined: the frequency of the bulk oscillation (ω_0) must be larger than the asymptotic frequency of the (antispiral) wave (ω_k), i.e., $|\omega_0| > |\omega_k|$.

It has been speculated that, similar to spiral waves, antispiral waves might occur in cardiac tissue [3]. However, this work suggests that it is unlikely that antispiral waves could form in the heart, where the underlying dynamics are excitable and far from the Hopf bifurcation. Alternatively, given that the percolation effect observed in the BZ-AOT system prevails in prolonged geological evolution, those centers where inwardly rotating, percolation-driven antispiral waves annihilate may serve as the substrate for depositing precious metals such as copper or uranium (see [28] and the references therein).

This work was supported by the American Heart Association (0030028N). We thank Calin Cuiianu for programming assistance.

*Electronic address: dchristi@med.cornell.edu

- [1] M. C. Cross and P. C. Hohenberg, *Rev. Mod. Phys.* **65**, 851 (1993).
- [2] A. T. Winfree, *Chaos* **1**, 303 (1991).
- [3] V. K. Vanag and I. R. Epstein, *Science* **294**, 835 (2001).
- [4] V. K. Vanag and I. R. Epstein, *Phys. Rev. Lett.* **87**, 228301 (2001).
- [5] V. K. Vanag and I. R. Epstein, *Phys. Rev. Lett.* **88**, 088303 (2002).
- [6] Y. X. Zhang, P. Foerster, and J. Ross, *J. Phys. Chem.* **96**, 8898 (1992).
- [7] V. S. Zykov, *Biophysics* **25**, 906 (1980).
- [8] J. P. Keener, *SIAM J Appl. Math.* **46**, 1039 (1986).
- [9] R. A. FitzHugh, *Biophys. J.* **1**, 445 (1961).
- [10] A. M. Pertsov, J. M. Davidenko, R. Salomonsz, W. T. Baxter, and J. Jalife, *Circ. Res.* **72**, 631 (1993).
- [11] W. H. Press, S. A. Teukolsky, W. T. Vetterling, and B. P. Flannery, *Numerical Recipes in C* (Cambridge University Press, Cambridge, U.K., 1992), 2nd ed.
- [12] A. M. Pertsov, M. Wellner, and J. Jalife, *Phys. Rev. Lett.* **78**, 2656 (1997).
- [13] M. Wellner and A. M. Pertsov, *Phys. Rev. E* **55**, 7656 (1997).
- [14] Y. Kuramoto, *Chemical Oscillations, Waves, and Turbulence* (Springer-Verlag, Berlin, 1984).
- [15] I. V. Biktasheva, *Phys. Rev. E* **62**, 8800 (2000).
- [16] M. Ipsen, L. Kramer, and P. G. Sørensen, *Phys. Rep.* **337**, 193 (2000).
- [17] S. Komineas, F. Heilmann, and L. Kramer, *Phys. Rev. E* **63**, 011103 (2000).
- [18] In Ref. [17], the term *antispiral* was used in a different context (to denote counterclockwise spiral-wave chirality).
- [19] Movies of the birth and propagation of antispirals can be downloaded at <http://www-users.med.cornell.edu/~dchristi/antispiral>.
- [20] From the generalized eikonal equation [Eqs. (9) and (31) of Ref. [13]], the condition for the occurrence of antispirals is $d|\Omega_k|/dk < 0$, which is consistent with what was found in Ref. [5]. For the CGL system, it is easy to prove that $d|\Omega_k|/dk < 0$ is essentially equivalent to the condition $|\Omega_0| > |\Omega_k|$ given in the text.
- [21] P. S. Hagan, *SIAM J. Appl. Math.* **42**, 762 (1982).
- [22] As the Benjamin-Feir instability criterion $1 + \alpha\beta < 0$ [1,14,16] is not satisfied, plane waves remain stable in this case.
- [23] M. Ipsen, F. Hynne, and P. G. Sørensen, *Int. J. Bifurcation Chaos Appl. Sci. Eng.* **7**, 1539 (1997).
- [24] R. J. Field, E. Körös, and R. M. Noyes, *J. Am. Chem. Soc.* **94**, 8649 (1972).
- [25] J. J. Tyson and P. C. Fife, *J. Chem. Phys.* **73**, 2224 (1980).
- [26] J. J. Tyson and J. P. Keener, *Physica (Amsterdam)* **32D**, 327 (1988).
- [27] *Oscillations and Travelling Waves in Chemical Systems*, edited by R. J. Field and M. Burger (Wiley, New York, 1985).
- [28] P. J. Ortoleva and S. L. Schmidt, in Ref. [27], pp. 333–418.